BUILDING A UNIQUE TEST SECTION FOR LOCAL CRITICAL HEAT FLUX STUDIES IN LIGHT WATER REACTOR – LIKE ACCIDENT CONDITIONS

Matkovič M.*, Cizelj L., Kljenak I., Končar B., Mikuž B., Sušnik A., Tiselj I., Zajec B.
*Author for correspondence
Reactor Engineering Division,
Jožef Stefan Institute,
1000 Ljubljana
Slovenia,
E-mail: marko.matkovic@ijs.si

ABSTRACT

Critical heat flux (CHF) has been studied for almost a century and yet there is no indisputable consensus reached on governing physical phenomena behind, not to mention, on modelling agreement of different correlations. When we are compelled to run our system at the safe distance from the CHF, and we can use all the accumulated knowledge so far, we will quite possibly cling to look-up tables delivered with that particular system. If this is not the case, than we will certainly stick to the system-specific correlation, which cannot be applied with confidence elsewhere. In the last two decades there were significant advancements applied both in numerical simulation capabilities and in unintrusive measuring techniques, which shed light on anticipated advancements in modelling the phenomenon. However, there are few reliable experimental measurements of instantaneous velocity and temperature fields in the wall boundary layer, and they are nil where local heat transfer coefficients are acquired. Therefore, at Reactor Engineering Division of Jožef Stefan Institute, a unique test section for local critical heat flux studies is under construction. The selected geometry and the test conditions will resemble light water reactor – like accident conditions. Moreover, to understand the phenomenon better, the design of the test section enables local measurements of heat transfer coefficients, and allows for control over the diabatic wall temperature. Measurements of single-phase convective heat transfer, conjugate heat transfer, flow boiling, convective condensation, and condensation-induced liquid hammer were all part of the test section's design basis. In this context, the design and construction of the device is herein presented in considerable detail.

INTRODUCTION

An accurate prediction of the convective single- and two-phase heat transfer is very important in process and power engineering for reliability, security, and efficiency of related systems and devices. There, heat is often transferred via flow boiling mechanisms, which is characterized by rather small and constant wall to fluid temperature difference, owing to the high heat transfer coefficient (HTC) and significant amount of latent heat stored in the changing phase respectively. However, the characteristic drawback of the boiling process is hidden in a distinct maximum of the heat transfer capability, followed by abrupt drop in heat transfer coefficient leading to escalation of the diabatic wall temperature. Usually, there is no other way around, to restore HTC, but to reduce the imposed heat flux, which presents a threat for the construction integrity of the components, like fuel elements, where internal heat generation responds with certain inertia.

There are essentially two main concepts of generating vapor for electricity production in light water nuclear power plants. In the first, vapor is generated directly in the reactor core, while in the second, steam generators are applied to transfer heat to the secondary fluid by its vaporization. In either case, and in all the system components, the heat flow rate density must always be kept far below the critical heat flux (CHF) margin. A substantial number of experimental studies, theoretical and numerical modelling of CHF has been published in the last seven decades or so. Reviews that focus on various aspects of the subject are published regularly [1]-[5], [9], [10]. In the past, the research was propelled mostly by the nuclear industry, while lately, the phenomenon has gained quite some interest also in the field of electronics cooling and compact heat exchangers with applications to mini-channels [6]. Installations, such as an array of micro thermocouples embedded in the wall and a set of optical probes installed in the fluid [7], allowed researchers to obtain measurements along the entire boiling

NOMENCLATURE

c	[J kg^{-1} K^{-1}]	Specific heat capacity
d	[m]	Tube diameter
HTC	[W m^{-2} K^{-1}]	Heat transfer coefficient
K	[W K^{-1}]	Heat loss coefficient (characteristic for a given setup)
$\dot{m}$	[kg s^{-1}]	Mass flow rate
q'	[W m^{-2}]	Heat flux
r	[J kg^{-1}]	Latent heat of vaporization
T	[K]	Temperature
x	[ ]	Vapor quality
z	[m]	Axial distance
Z	[m]	Active length of the test-section

Subscripts

e	External
f	Fluid
p	Pressure
sat	Saturation
w	Water – Secondary fluid

curve; including CHF. Adoption of non-intrusive measuring techniques followed and the researchers have measured instantaneous velocity fields and turbulence intensities deep in the wall boiling boundary layer [8], on the scale where only few dared to dream of. Many have studied nanofluids [9] and the key surface factors [10] while looking for responsible mechanisms and striving for CHF enhancement, and yet, the origin of the CHF remains obscure to scientific community. Indeed, there is still no indisputable consensus reached on governing physical phenomena behind the occurrence of the critical heat flux, which inherently results in different modelling approaches of the phenomenon.

The advancement in the CHF understanding is rather slow. Apart from the fact that CHF is ruled by a set of complex physical mechanisms, part of the reason for the slow progress must also be attributed to predominant specialisation of different research groups, which often limit themselves to either the analytical, numerical or the experimental work. Where needed, they will rely on other's people work, which is usually not updated to the studies of their own interest.

In this light, one of the motivations behind the construction of the new experimental device was to put together the needed research infrastructure and, in one place, link together theoretical efforts, numerical simulations and experiments. In this way each phenomenon could be studied from different perspectives all over again until one reaches a sound understanding of the responsible mechanisms behind, which only then become subject for modelling.

THE EXPERIMENTAL APPARATUS

During the first step of the planning phase, we prepared a list of desired boundary test conditions, a wish list, for the experiment. On one hand, we strived for the widest possible range of test conditions, while on the other hand, there were inherent constraints imposed by the given infrastructure, resources and by the commitment to perform experiments at the highest accuracy levels. Indeed, care to maintain high quality measurements has been taken into account in every design aspect of the apparatus. Once the boundary conditions for the test apparatus had been set, high quality instruments were installed in the rig. A list of typical experimental test conditions and the associate uncertainties are shown in Table 1.

Design process and constraints of the test apparatus

The design process of the test apparatus was very much governed by a set of given constraints and a list of our wishes. Table 2 summarizes the main effects the design process had on the construction of the apparatus. The request for wide range of reduced pressures, for example, declined water to be applied in the primary loop and gave priority to studying various fluids instead. The request for isothermal boundary conditions necessitated another important design feature of the apparatus; the use of the secondary fluid, which allows for better control over the diabatic wall temperature. The same feature is also essential for studying CHF at controlled wall temperature instead of at imposed heat flux.

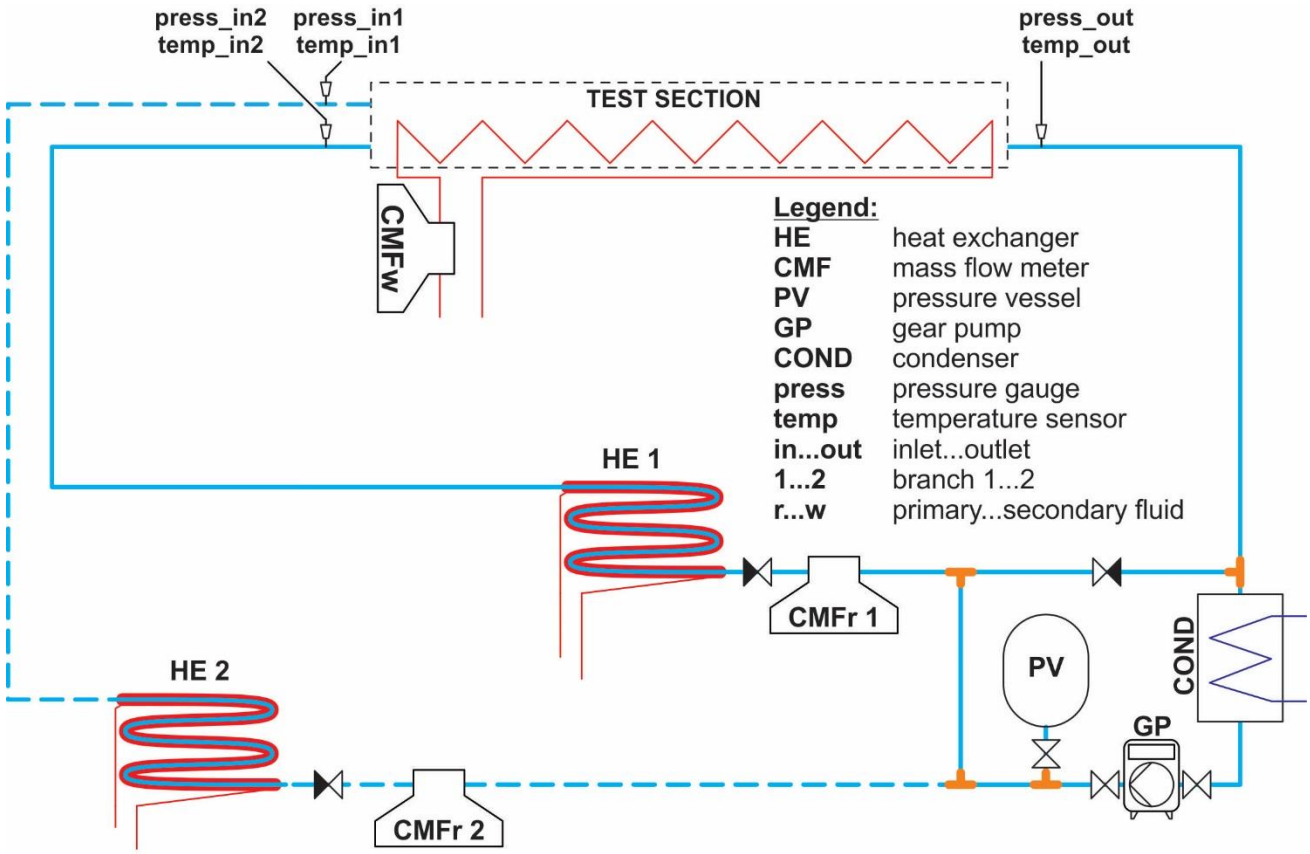

Figure 1 Schematic of the experimental test apparatus.

Table 1 A list of typical experimental test conditions and the associated uncertainties.

Boundary condition	Typical Value	Comment
Temperature range	from 5°C to 90 °C when water is used	± 0.05 °C … (regularly calibrated onsite)
*Prim. Fluid Flow Rate - max	440 kg h^{-1} ...MGP (CMFr1+ CMFr2)	± 0.44 kg h^{-1} (± 0.1 % of the measured value)
Prim. Fluid Flow Rate - min	1.83 kg h^{-1} ...CMFr2 (1/60 of span)	± 0.0037 kg h^{-1} (± 0.2 % of 1/60 of the span)
Water Flow Rate - max	1770 kg h^{-1} ...CMFw3	± 1.77 kg h^{-1} (± 0.1 % of the measured value)
Water Flow Rate - min	5.5 kg h^{-1} ...CMFw4 (1/60 of span)	± 0.011 kg h^{-1} (± 0.2 % of 1/60 of the span)
Water Temp. Difference	2 °C - 20 °C …4-junction thermopile	± 0.03 °C (calibrated onsite)
Wall-Ref. Temp. Diff.	2 °C - 10 °C …2 thermocouples	± 0.1 °C
Pressure	up to 20 bar …system pressure (MGP head)	± 1.25 kPa (0.05% of span - 25 bar)
Pressure Difference	0.1 bar ...	± 0.01 kPa (0.1% of span - 0.1 bar)
Wall Surface Temperature Distribution	< 0.03 °C (spectral range: 7.5-9 μm) at 640x512 ... IR camera	high sensitivity to local temperature variations

*Coriolis-effect mass flow meters are used for mass flow rate measurements of the primary fluid and water

THE TEST SECTION

The test section was designed for experimental heat transfer and fluid flow studies during single-phase flow, convective condensation, flow boiling and critical heat flux. However, only aspects relevant to critical heat flux studies are herein discussed.

The defined boundary conditions have set both the overall characteristics of the test rig and the geometrical constraints of the test section. In fact, the latter was primarily defined with the use of the secondary fluid-water, limited to around 10 kW of heating power and with the desired fluid's mass velocity of around 2000 kg m^{-2} s^{-1} within the annulus. In this context, a short calculation proved that external tube diameter of 12 mm with integrated heat exchanger inside was found as a good compromise for the annular test section resembling a fuel rod geometry.

Table 2 A wish list and constraints affecting the design of the test apparatus.

Wishes and constraints	The decisions
Q = 10 kW (for heating) G = 2000 kg $m^{-2}s^{-1}$	d_h < 5.6 mm
Running experiments in wide range of reduced pressures	Use of different fluids (water is excluded)
Isothermal boundary conditions	Adoption of secondary fluids
Resembles nuclear fuel rod geometry	External flow (flow in the annulus with heated cylinder)
Advanced visualization of the process	Transparent cover/envelope (for visible and IR spectra)
Local HTC measurements	Local wall temperature and heat flux measurements
Flow boiling studies	Heating of the rod surface
Local CHF studies	Controlled wall temperature
Convective condensation	Cooling of the tube surface
Possibility of surface treatment, changing inserts (turbulence promoters, phase separation…)	Dismountable device

Similar calculation has shown that the length of around 700 mm was found sufficient to allow for the set heating power be transferred to the primary fluid. Lightly subcooled or saturated liquid, entering the annulus, will boil and, if the wall is sufficiently superheated, it will reach the departure from nucleate boiling (DNB) conditions. The length of the test section was calculated for the target thermal power of 1 kW, cumulative water temperature drop of 10 K, allowable pressure drop of 1 bar on the secondary side, and overall vapor quality change of 5 %. The water path through the rod was carefully designed to allow for adequate mixing, while at the same time not obstructing the flow over the selected length beyond the targeted pressure drop.

Low experimental uncertainty integrated into the design

The test section has been a priori designed with view to acquire data at the highest possible accuracy level. In this context, several aspects have been carefully integrated into the design of the test section.

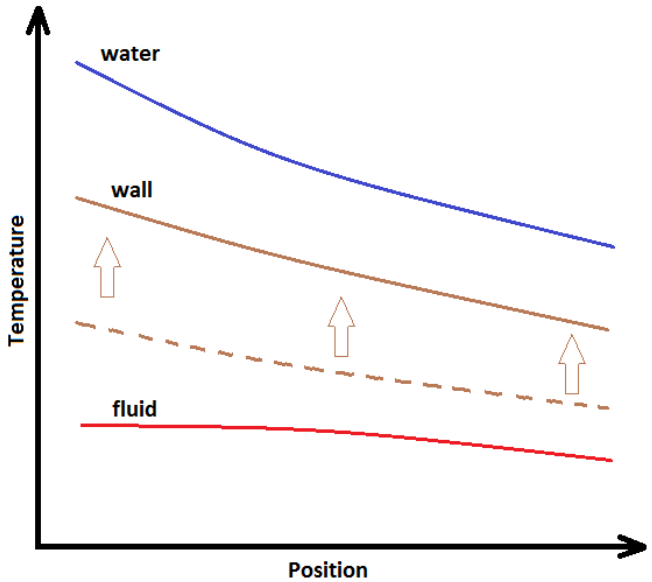

Figure 2 Schematic representation of the effect of the reduced thermal resistance on the secondary side.

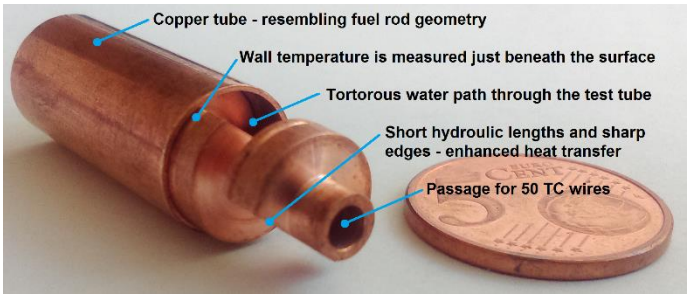

Figure 3 Insight into the water path and the enhanced heat transfer surface within the tube resembling fuel rod geometry.

First, special care was taken to reduce thermal resistance on the secondary side (Figure 2) as much as reasonable. There, the short hydraulic lengths and sharp edges form a torturous path on the secondary side (Figure 3), which enable nearly perfect mixing of the fluid with constantly interrupted boundary layer that will in turn result in significantly higher heat transfer coefficient. Decreasing thermal resistance on the secondary side will move the measured wall temperature closer to the secondary fluid temperature. Therefore, the increased wall superheat will reflect in reduced uncertainty during the HTC measurements. The heat transfer enhancement is particularly important during flow boiling studies or convective condensation tests where high heat transfer coefficients are expected on the primary side.

Second, performing local measurements of critical heat flux at controlled wall temperature and reduced experimental uncertainty required specific approach. In this respect, authors adopted a particular technique that has been successfully applied by Cavallini and co-workers [11] at their studies of local heat transfer coefficients inside the single minichannel. The technique is described further on.

Third, even though the test section is designed in a way that measurements need very little or no corrections to be accounted for, a number of modifications will be integrated in data acquisition and post processing phase. Here, analytical deductions and assessments from detailed numerical simulations will all be taken into account. For example, diabatic wall temperature is measured just beneath the surface. High thermally conductive material – copper is used to cause as small temperature gradients as possible, and yet, there is heat flux dependent temperature drop between the measured and the target location, which needs to be accounted for in the given geometry.

Fourth, an important feature of the test section is a collector where both fluids are supplied into the test tube (Figure 4). Here, attention was payed to supply the primary fluid homogeneously into the annulus by keeping the dominant local pressure drop within the orifice realised with multiple holes.

Fifth, once the overall dimensions were set, a standard polycarbonate tube with appropriate internal dimensions was found a suitable transparent outer wall of the annulus. Particular attention was payed to keep the thickness of the polycarbonate tube thin since transmittance for IR spectra may be significantly affected at higher thickness (Figure 5). In order to cope with the designed test conditions, the tube was reinforced with two layers of fibreglass laminate to prevent it from creeping and shattering at higher temperature and pressure.

Sixth, the thickness of the test section tube had to be defined with care. On one hand one has to fight against axial heat conduction through the wall, while on the other hand, homogeneous heat flux and thus surface temperature distribution is required on the diabatic surface. The homogeneity of the wall surface temperature will be eventually controlled with an infrared camera during single-phase heat transfer studies with superheated vapor running inside the annulus. On the other hand, the correction from axial contributions can not be measured directly, but it will be accounted for during data acquisition and post processing (Figure 6 B, eq. 4). The overall correction of the described local heat transfer is expected to be in the range of 2 % during flow boiling studies. However, this value becomes significantly more pronounced when CHF with abrupt drop in HTC is studied (Figure 6).

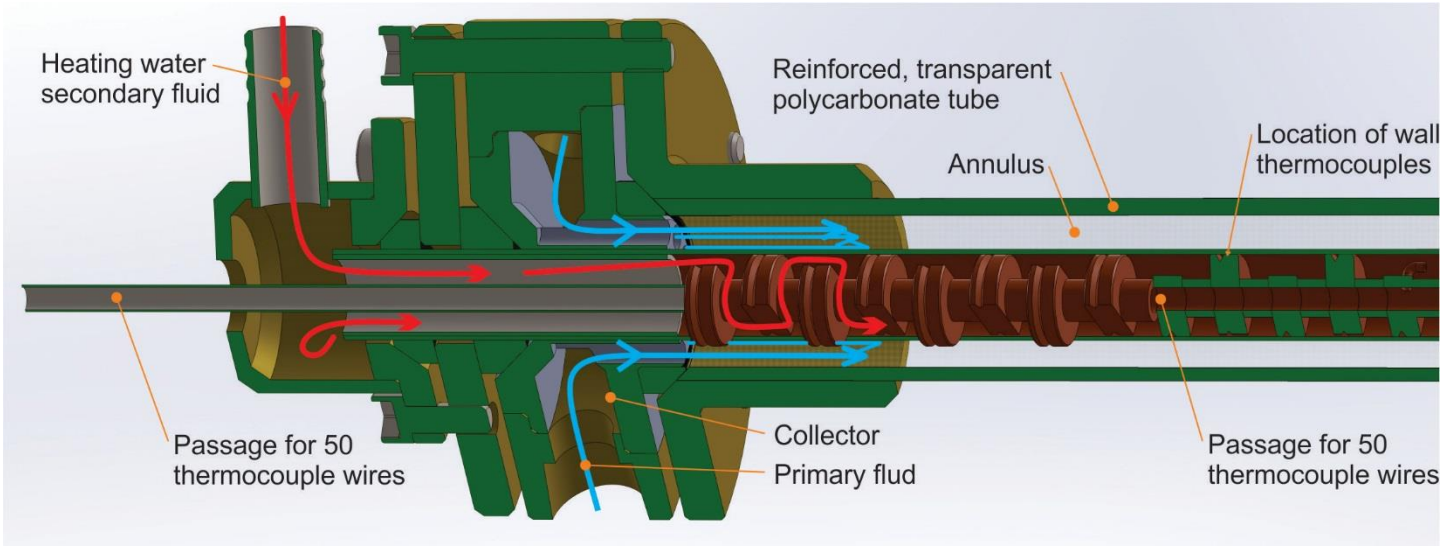

Figure 4 Insight into the test section inlet.

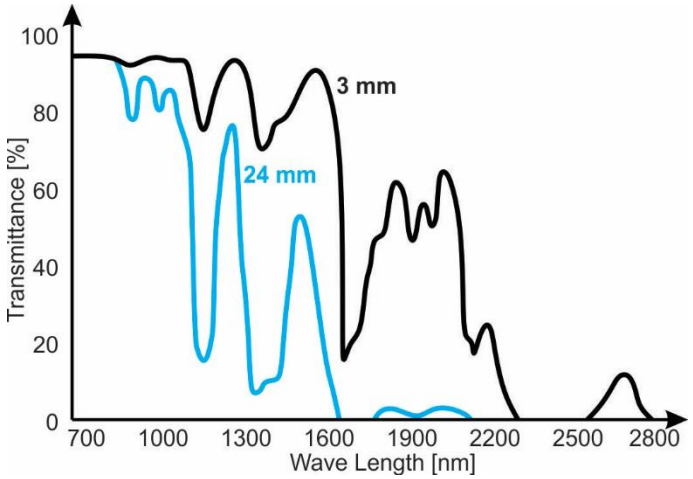

Figure 5 Infrared transmittance of polycarbonate tubes with two different wall thicknesses.

Flow boiling and CHF tests

During the flow boiling and CHF experiments, the secondary fluid, water, will run in co-current flow through the test section where heat is transferred to the primary fluid. There, the temperature profiles of both fluids are decreasing along the flow path. The first temperature decrease arises from the decreasing internal energy, due to heat transfer, while the second decrease originates from the overall pressure loss and thus the saturation temperature drop. Here, all three origins of pressure loss must be taken into account: friction, momentum change and gravity that are namely associated to the realistic flow of viscous fluid, evaporation and vertical installation of the test section respectively. During the test, the wall temperature will keep decreasing until the occurrence of the CHF. At that point, it will approach the water temperature profile, which will both level off in a rapid manner. Calculation of the fluid temperature will, however, be subject of a more complex modelling and calculation.

NUMERICAL METHOD

In order to measure the local heat transfer coefficients at the same location where the velocity field in the near wall region will be acquired instantaneously, authors adopted and combined two techniques. The first one has been successfully applied by Cavallini and co-workers at their local heat transfer studies inside the single minichannel [11], while the second one; the PTV experiments have been performed in the near-wall region by Estrada-Perez and Hassan [8]. Heat transfer coefficient defined as:

$$HTC(z) = \frac{q'(z)}{T_{fluid}(z) - T_{wall}(z)}, \qquad (1)$$

requires local heat flux and wall to fluid temperature difference measurements. The first can be obtained from the accurate measurements of the water flow rate and local fluid temperatures along the test tube. Knowing also the geometry of the test section, local heat flux can be calculated as follows:

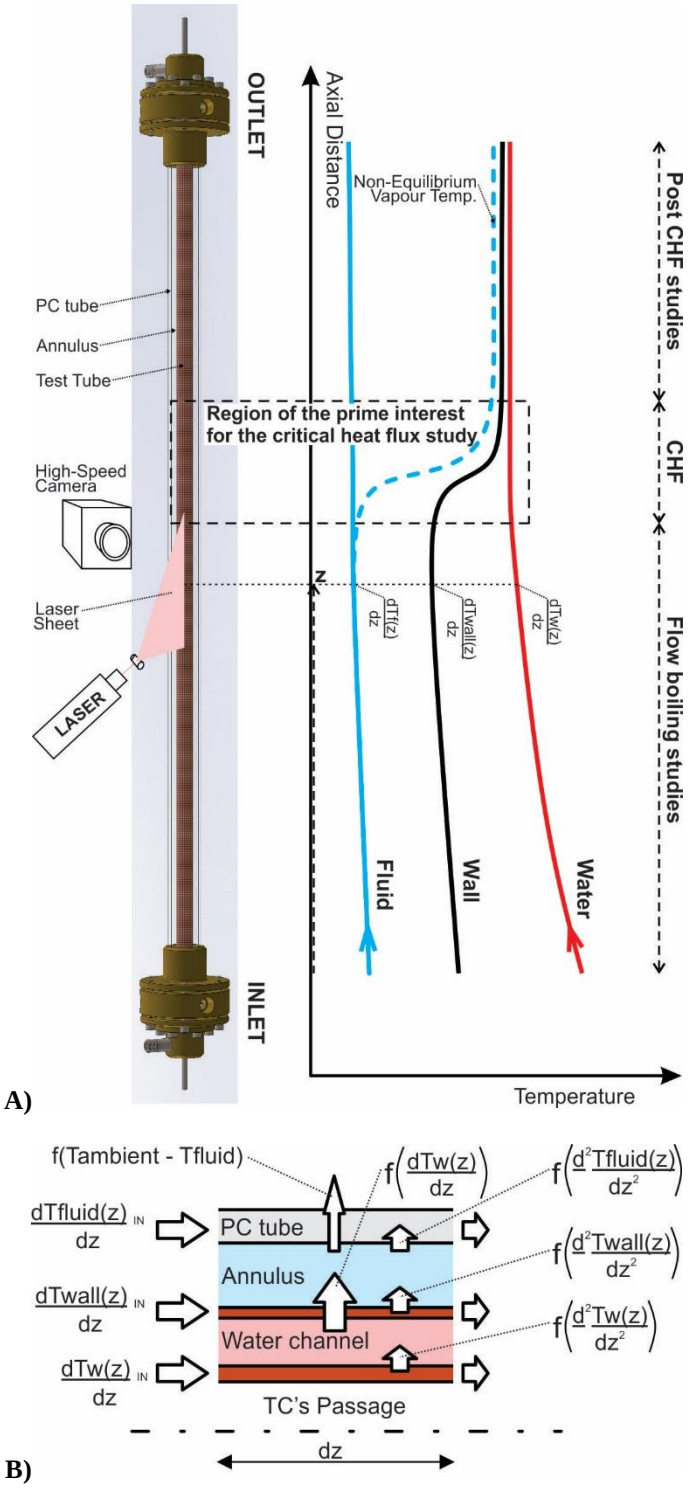

Figure 6 A) Expected water, wall and fluid temperature profiles during flow boiling studies with occurrence of CHF along the test section. Schematic setup of the measuring device for velocity field and liquid-vapor interface tracking is also shown in the figure by means of a laser and a high-speed camera installation along the test section axis.
B) Schematic representation of the temperature gradient variation along the test tube.

$$q_0'(z) = \dot{m}_w \cdot c_{pw} \cdot \frac{1}{\pi \cdot d_e} \cdot \frac{dT_w(z)}{dz} \quad . \tag{2}$$

To account also for the thermal losses and the effect of temperature gradient variation along the test section, several corrections have to be taken into consideration during calculation of the local heat flux. Good estimation of the thermal losses can be obtained from the adiabatic single-phase runs performed at various fluid to ambient temperature differences. From the obtained characteristic curve of the overall heat losses with the K_{loss} for a given test section's setup one can deduce local heat losses that affect the local heat flux calculation.

$$q'_{loss}(z) = \frac{K_{loss}}{\pi \cdot d_e \cdot Z} \cdot \left(T_{amb} - T_{fluid}(z)\right) \tag{3}$$

Another set of corrections comes from the axial heat conduction through the construction elements of the test section (Figure 6 B). These contributions are particularly important once sharp variations in temperature gradients are measured, i.e., when approaching the region of the prime interest for the CHF study. Local heat flux is therefore calculated as follows:

$$q'(z) = q_0'(z) + q'_{passage}(z) + q'_{wall}(z) + q'_{PCtube}(z) + q'_{loss}(z) \quad . \tag{4}$$

Finally, the integral value of heat transferred to the primary fluid over the length *z*:

$$Q(z) = \pi \cdot d_e \cdot \int_0^z q'(z) \cdot dz \tag{5}$$

is used to calculate the local vapor quality:

$$x(z) = x_{in} - \frac{Q(z)}{\dot{m}_f \cdot r} \quad . \tag{6}$$

The overall heat transfer within the test section will also be continuously controlled with the measured temperature difference between the water inlet and outlet.

CONCLUSION

Heat transfer systems, such as water nuclear reactors, must avoid the occurrence of critical heat flux by all means, as the phenomenon is associated to sudden decrease of heat transfer coefficient and uncontrolled increase of wall temperature that may eventually lead to the system failure. Good understanding and reliable prediction of the said phenomenon is of paramount importance for reliable, secure, and efficient operation of selected systems related to process and power engineering. In order to confront the scarce understanding of the critical heat flux phenomenon head on, more research has to be done in this respect. In this context, a unique test section for local critical heat flux studies has been designed and is being built at Reactor Engineering Division of Jožef Stefan Institute. To understand the governing physical mechanisms of the CHF better, the test section has been designed so as to allow for local measurements of the heat transfer coefficients at controlled diabatic wall temperature, while at the same time, enables the insight into the instantaneous velocity field within the wall boundary layer. The design of the test section and the test conditions, which will resemble light water reactor – like accident conditions is herein presented in considerable detail. Particular emphasis was put onto profound studies within the wall boundary layer, where most of the heat and momentum transfer take place. There, a reliable CFD model must be consistent for every cell as information is passed from one cell to another. Indeed, the same bulk averaged values may result in substantially different local thermal-hydraulic conditions that would eventually lead to important variations in CHF calculation. Results from the designed test section will therefore enable better understanding and reliable mechanistic and CFD model developments.

REFERENCES

[1] Celata G.P., Cumo M., Mariani A., Simoncini M., Zummo G., 1994, Rationalization of existing mechanistic models for the prediction of water subcooled flow boiling critical heat flux, Int. J. Heat & Mass Transfer, vol. 37, pp. 347-360.

[2] Sadasivan P., Unal C., Nelson R., 1995, Perspective: issues in CHF modelling – the need for new experiments, J. Heat Transfer, vol. 117, pp. 558-567.

[3] Hall D.D., Mudawar I., 2000a, Critical heat flux (CHF) for water flow in tubes. I: Compilation and assessment of world CHF data, Int. J. Heat & Mass Transfer, vol. 43, pp. 2573-2604.

[4] Hall D.D., Mudawar I., 2000b, Critical heat flux (CHF) for water flow in tubes. II: Subcooled CHF correlations, Int. J. Heat & Mass Transfer, vol. 43, pp. 2605-2640.

[5] Roday A.P. and Jensen M.K., 2009, A review of the critical heat flux condition in mini-and microchannels, Journal of Mechanical Science and Technology, vol. 23, pp. 2529-2547.

[6] Mastrullo R., Mauro A.W., Thome J.R., Vanoli G.P., Viscito L., 2016, Critical heat flux: Performance of R1234yf, R1234ze and R134a in an aluminum multi-minichannel heat sink at high saturation temperatures, International Journal of Thermal Sciences, vol. 106, pp. 1-17.

[7] Auracher H., Marquardt W., 2004, Heat transfer characteristics and mechanisms along entire boiling curves under steady-state and transient conditions, Int. Journal of Heat and Fluid Flow, vol. 25, pp. 223-242.

[8] Estrada-Perez, C.E., Hassan, Y.A., 2010, "PTV experiments of subcooled boiling flow through a vertical rectangular channel", Int. J. Multiphase Flow, vol. 36, pp. 691-706.

[9] Fang X., Chen Y., Zhang H., Chen W., Dong A., Wang R., 2016, Heat transfer and critical heat flux of nanofluid boiling: A comprehensive review, Renewable and Sustainable Energy Reviews, vol. 62, pp. 924-940.

[10] Mori S., Utaka Y., 2017, Critical heat flux enhancement by surface modification in a saturated pool boiling: A review, International Journal of Heat and Mass Transfer, vol. 108, Part B, pp. 2534-2557.

[11] Cavallini A., Bortolin S., Del Col D., Matkovič M., Rossetto L., 2007, Experiments on dry-out during flow boiling in a round minichannel, Microgravity sci. technol., vol. 19, no. 3/4, pp. 57-59.